Reduction of nitrate and ammonium adsorption using microscale iron particles and zeolitite

(Article begins on next page)

29 June 2024

The final publication is available at Springer via http://dx.doi.org/10.1007/s11270-011-0926-2

Reduction of nitrate and ammonium adsorption using microscale iron particles and zeolitite

Silvia Comba[a], Maria Martin[b], Daniele Marchisio[a], Rajandrea Sethi[a], Elisabetta Barberis [b]

[a] DITAG – Dipartimento del Territorio, dell'Ambiente e delle Geotecnologie, Politecnico di Torino, Torino, Italy.

[b] Di.Va.P.R.A. - Dipartimento di Valorizzazione e Protezione delle Risorse Agroforestali, Facoltà di Agraria, Università di Torino, Italy

Corresponding Author: Rajandrea Sethi, rajandrea.sethi@polito.it

1. Abstract

Nitrate contamination of groundwater represents a treat to human health. Many researchers have studied zerovalent iron as a mean to remediate nitrate contamination. However the application of such method is limited by ammonium production. This work investigates the use of microscale iron particles in association with zeolitite, a natural material containing zeolite, to remove nitrate and ammonium from groundwater. The association of the two materials is shown to lower nitrate concentration in both deionized and groundwater under the limit suggested by the European Union and to significantly reduce the ammonium concentration. The method is potentially applicable in water filtration.

2. Keywords: 1. micrometric iron 2. nitrate, 3. zeolitite, 4. groundwater, 5. water filtration.

3. Introduction

The presence of nitrate in drinking water represents a problem due to its harmful biological effects. High dietary intakes of nitrate and nitrite can cause methemoglobinemia (Liang B. C., 1994), and

have been implicated in the etiology of human gastric cancer based on epidemiology and clinical studies (Bartsch *et al.*, 1990), (Joossens *et al.*, 1996).

Nitrate contamination of groundwater is widespread mainly due to the leaching of nitrogen fertilizers used in agriculture to intensive animal breeding, food processing, industrial waste effluent discharge (Follett, 2001) and to the leaching of septic tanks (Hallberg, 1993). The concentration of nitrate in groundwater often exceed the European standard for nitrate in drinking water of 10 mg/l nitrate-N (European Council, 2001) in several European areas subjected to intensive agricultural practices and where soils have a poor protection capacity for the water table, such as some zones in the Po valley, Italy. The situation is exacerbated in rural areas of the developing world where the inputs of nitrogen to agricultural soils are increasing and no centralized drinking water system is available. Therefore efficient and affordable methods for safe drinking water production should be available, both at household and at small and big community level (Noubactep and Caré; Shannon *et al.*, 2008; Sobsey *et al.*, 2008).

The use of zerovalent iron has been proposed for reduction of nitrate (Alowitz and Scherer, 2002), (Westerhoff and James, 2003), (Zawaideh and Zhang, 1998), (Chew and Zhang, 1998):

$$NO_3^- + 4Fe^0 + 10H^+ \longleftrightarrow NH_4^+ + 4Fe^{2+} + 3H_2O$$
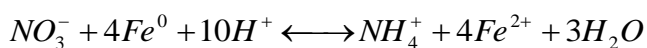
Eq. 1
This reaction has been exploited in situ, by realizing Permeable Reactive Barriers (PRB) using millimetric iron (Gu, 2002). PRBs are typically constructed via trenching and excavation (Molfetta and Sethi, 2006).

Many studies have been conducted on nitrate reduction by millimetric (Buresh, 1976), (Westerhoff and James, 2003), Su and Puls (2004, 2007), (Rodriguez-Maroto *et al.*, 2009), micrometric (Schaefer *et al.*, 2007), (Huang *et al.*, 1998), and nanoscale iron (Schaefer *et al.*, 2007), (Liou *et al.*, 2005), (Choe *et al.*, 2000), (Chen *et al.*, 2004), (Yang and Lee, 2005), (Li *et al.*, 2006), (Sohn *et al.*,

2006), (Shin and Cha, 2008), (Liou *et al.*, 2006). Most of the above mentioned works investigated the reactions' kinetic, whereas little attention has been devoted to the system in thermodynamic equilibrium.

Almost all studies convey that ammonium is the main reaction product, even if some of them report nitrite as intermediate species (Rahman, 1997) and (Siantar *et al.*, 1996) and one study on nanoscale iron reports nitrogen gas to be the only reaction product (Choe *et al.*, 2004). The ammonium ion is an undesired species in groundwater mainly because it can lead to nutrient enrichment of water systems and subsequently to eutrophication, and because it determines taste and odour problems in drinking water (Huang *et al.*, 2000). Therefore the production of ammonium may be a drawback for field application of nitrate reduction by iron.

Zeolites are an important class of materials which are characterized by a three-dimensional framework structure with uniform pore and channel systems, where exchangeable cations can be accommodated. Deposits of zeolitites, natural materials containing zeolite, are diffused in several zones of Italy. Chabasite is one of the most common constituents in Italian natural zeolitite deposits, and exhibits a high affinity for NH_4^+ ion (Passaglia, 1999) and (Passaglia, 2008). The use of zeolite has been proposed for ammonium removal from groundwater (Wang *et al.*, 2008).

The reductive capacity of Fe^0 towards nitrate could be favourably combined with the adsorbent properties of zeolitites, as proposed by Lee et al., 2007, who synthesized a nanostructured material derived from zeolite modified with Fe(II) subsequently reduced to Fe^0. The material is able to rapidly reduce nitrate without ammonium release under unbuffered pH, however, it is not presently commercially available for large scale application. The combination of zerovalent iron and natural zeolitites for the removal of nitrate and ammonium could be practically feasible and cost effective, although the effectiveness of this combination has still to be proved.

Most studies focus on kinetic considerations. However (Sohn *et al.*, 2006) points out the importance of evaluating also the amount of iron which is consumed in the reaction, in order to reach a complete nitrate reduction and, contemporarily, to avoid leaving part of the material unexploited.

The primary end points of this study are to determine the dosage of micrometric iron needed for the complete nitrate reduction (i.e. the amount of nitrate that can be reduced per mass unit of iron introduced in the aquifer) and to evaluate the feasibility of using zeolitite to remove ammonium after nitrate reduction by micro iron particles. Experiments were conducted in both synthetic and groundwater in order to evaluate the influence of different cations and anions naturally occurring in groundwaters on the reduction reaction of nitrate by Fe^0.

3. Experimental section

3.1 Materials characterization

Reactive micro scale zero-valent iron was provided by Basf, in form of carbonyl iron powder commercially known as SM micro. According to the producer, the Fe content of the material is > 99%, while particles dimension is below 10 μm ($d_{10\%}$=2.1, $d_{50\%}$=3.5, $d_{90\%}$=5.5). The zeolitite was provided by Sorano mines, in Central Italy. The chemical and physical properties of this zeolitite are described by Passaglia (2008). The contained zeolites were 66% Chabasite and 1.4 Phillipsite. According to Passaglia (2008) the C.E.C of the zeolitite is 2.17 $mol_c\,kg^{-1}$ and the naturally occurring exchangeable cations are mainly Ca (1.46 $mol_c\,kg^{-1}$) and K (0.60 $mol_c\,kg^{-1}$). To minimize material heterogeneity we used the <0.5 mm fraction of zeolitite.

Experiments of nitrate reduction were conducted both in deionized water spiked with a nitrate salt ($NaNO_3$, Sigma Aldrich) and in a groundwater, sampled near the city of Fossano in Piemonte Region, North West of Italy. This sampling site is representative of the groundwater characteristics of a wide area in the Western Po valley subjected to intensive agricultural and farming activities,

coupled with a scarce soil capacity to protect groundwater from nitrate leaching, thus increasing the risk of contamination.

The nitrate concentration was adjusted to the desired value by adding $NaNO_3$ (Sigma Aldrich). Surface morphologies of unreacted iron powder, iron after reaction with nitrate and of the iron-zeolitite mix were obtained by a field emission scanning electron microscope (FE-SEM, Hitachi S-4700) equipped with a Gemini Field Emission Column, and an Energy Dispersive X-ray (EDX) probe (Low Vacuum Scanning Electron Microscope Quanta Inspect 200), that was used for semi-quantitative analysis of chemical composition. Samples were prepared by drying the powders at ambient temperature under atmospheric conditions.

The mineralogical features of the zeolitite sample were determined by X-ray diffraction using a Philips 1710 diffractometer (40 kV and 20 mA, Co-Kα radiation, with graphite monochromator). Scans were made from 2 to 50° 2θ at steps of 0.020° 2θ and 1 sec/step.

The concentration of the major anions in solution in groundwater was determined by ionic chromatography. The total dissolved organic carbon was determined by a Vario TOC Cube analyzer, Elementar (Hanau, Germany). Results are reported in Table S 1..

3.2 Abiotic reduction of nitrate by zerovalent iron

The influence of the interaction time on nitrate reduction was studied by batch experiments conducted in 100 ml airtight bottles sealed with a rubber plug. The Fe^0 concentration was 100 g l^{-1} and 33 mg l^{-1} N-NO_3^- were added. The experiment was performed both in deionized water and groundwater, with the same concentrations of Fe^0 and N-NO_3^-. Oxygen was removed by purging all the used solutions with argon, and the headspace of each sample bottle was filled with the same gas. Control experiments containing no Fe^0 particles were also prepared. Bottles were shaken on a reciprocating shaker (Glas-Col) at 60 rpm at 25°C in the dark. Aliquots of 5 ml were withdrawn at selected times using a plastic syringe and immediately filtered through a 0.2 μm filter.

Nitrate and nitrite concentrations in solution were determined by ion chromatography with a Dionex DX-500, 2 mm system, equipped with an auto-sampler AS50, AS4 analytical column, and AG4 pre-column. The eluent was 1.8 mM sodium carbonate/1.7 mM sodium bicarbonate pumped at a flow rate of 0.25 ml min^{-1}. Ammonium concentration was determined colorimetrically using the salicylate-dichloroisocyanurate reaction (Crooke, 1971). The dissolved Fe^{2+} concentration was determined colorimetrically using the orthophenantroline method (Loeppert and Inskeep, 1996).

A series of batch reduction experiments was also performed to evaluate the amount of iron which is consumed in the reaction, in order to optimize the dosages, ensuring a complete nitrate reduction while avoiding that part of the expensive material could remain unexploited. Therefore, various weighed amounts of iron (1, 5, 10 g) were introduced into 50 ml bottles with 50 ml solution containing 2, 12, 23, 33, 45 mg l^{-1} of N-NO$_3^-$. Both deionized water and groundwater were used. A contact time of 40 or 120 hours was used respectively for deionized water and groundwater (accordingly with the results of the previous step, in order to reach semi-equilibrium in the reduction reaction). Nitrate, nitrite and ammonium were measured as described above.

At the end of the experiment, values of oxidation-reduction potential (ORP) and pH were measured (WTW, Multi 340i probe). Nitrate, nitrite and ammonium are reported respectively as nitrate-nitrogen (N-NO$_3^-$), nitrite-nitrogen (N-NO$_2^-$), ammonium-nitrogen (N-NH$_4^+$).

3.4 Ammonium adsorption on zeolitite

Batch adsorption isotherms of ammonium removal by zeolitite were carried out in polyethylene bottles. Each bottle was filled with 50 ml of deionized water spiked with ammonium to reach a concentration ranging from 0.07 to 230 mg N-NH$_4^+$ l^{-1}, then 0.5 g of zeolitite were introduced into each bottle. Bottles were shaken on a reciprocating shaker at 25 °C for 4 h in the dark. Preliminary tests showed that within this time the equilibrium was reached. At the end of the interaction period,

the two phases were separated by filtration through a 0.20 μm membrane filter. The ammonium concentration remaining in solution was measured as described in the previous section.

Experimental data were fitted using the Freundlich isotherm:

$$Q = KC_e^{1/n}$$

Eq. 2

where Q is the amount of ammonium adsorbed per unit weight of zeolitite, C_e the concentration of ammonium remaining in the solution at equilibrium, K and n are empirical constants.

Adsorption of nitrate by zeolitite was also investigated with the same procedure by placing 33.5 mg N-NO$_3^-$ l^{-1} and 0.5 g of zeolitite in a volume of 50 ml.

After studying the reactive properties of iron and the adsorption capacity of zeolitite, the two materials were used together to assess the feasibility of ammonium removal from the solution through adsorption on zeolitite after nitrate reduction. A fixed amount (0.5 g) of zeolitite was introduced into each 50 ml bottle after the reaction between iron and nitrate. The iron dosage was equal to 100 g l^{-1}. The N-NO$_3^-$ concentration was 35 mg l^{-1} for deionized water and 20 mg l^{-1} for groundwater.

Statistical analysis was performed with the software Minitab. Averaged results from duplicate tests were reported. In general, relative sample standard deviations for duplicate tests were less than 12%.

4. Results and Discussion

4.1 Abiotic nitrate reduction by zerovalent iron: effect of interaction time

The iron concentrations over time (or ammonium production) are reported in Figure 1. The reaction showed a delay time of nearly 8 h both in deionized water and in groundwater, likely due to the

possible presence of oxygen traces in solution even after purging with Ar. Once the reaction started, nitrate was completely reduced within 48 hours in deionized water. In contrast, in groundwater the nitrate concentration decreased substantially more slowly, and the amount of reduced nitrate was smaller. Even after 10 days of interaction, some unreacted nitrate was still present in solution.

In both deionized and ground water, once the reaction had started, after a faster nitrate reduction step the reaction slowed down. In the case of groundwater, the change in the slope of the plot of the reduced nitrate (or the produced ammonium) vs time is more marked and can be noticed in correspondence of 86-100 hours, suggesting a sharp decrease in the reaction rate after 3-4 days of interaction (Figure 1).

The reduction of nitrate could be described by a pseudo-first-order equation, according to previous findings (Choe *et al.*, 2000), (Alowitz and Scherer, 2002), (Su and Puls, 2004). The values of the rate constants, determination coefficients and level of significance are summarized in Table 1. In the case of groundwater, the observed decrease in the rate of nitrate reduction after 86 h resulted in a change of the slope in the pseudo-first-order model (Figure S 1). The kinetic was thus split into a fast-reaction step (12h-86h) and slow-reaction step (86h-254h).

The pseudo-first-order rate constant determined for the nitrate reduction in distilled water was one order of magnitude greater than the rate constant determined for the fast step in groundwater, and the rate constant of the slow reaction step in groundwater was more than 4 folds smaller than that calculated for the fast step. The slow phase of the reduction reaction, in groundwater, was a long-lasting process, which was still going on after 16 days of interaction (data not shown).

A change in the rate constant is not unusual in the case of surface reactions, such as the reactions of specific adsorption or desorption of anions and cations on/from the surfaces of iron or aluminum oxides (Liu and Huang, 2003), (Saha *et al.*, 2004, 2005), (Yu *et al.*, 2006) and (Martin *et al.*, 2009). The chemical reduction of nitrate by zerovalent iron has been confirmed to be a surface-mediated

process (Weber, 1996) and (Rodriguez-Maroto *et al.*, 2009) and one of the main proposed rate-limiting factors, beside mass transport of nitrate to the iron surface, is the availability of reactive surface area on the iron particles (Yang and Lee, 2005), that could progressively decrease as the reaction proceeded. The decrease of the total amount of nitrate reduced at the end of the experiment and the slower kinetic of the process in groundwater compared with deionized water has been explained in the literature with the blockage of reactive sites on the surface of Fe^0 and its corrosion products by specific adsorption of inner-sphere complex forming ligands (such as oxalate, citrate, sulphate, borate, phosphate) (Su and Puls, 2004). The groundwater used in this study actually contained high concentrations of sulphate (Table S 1). Also carbonate anions, which are present in high levels in the used groundwater, can play a role in the reduction of the reactive sites, as they could form surface precipitates on the iron particles, diminishing the surface area available for nitrate reduction, thus decreasing the speed of the reaction (Westerhoff and James, 2003).

4.2 Abiotic nitrate reduction: effect of the amount of iron

Nitrate reduction in Deionized Water. Based on the results on the time experiments, a reaction time of 40 h was selected, to allow the reaching of quasi-equilibrium, as deduced by the kinetic experiments (Figure 1). The results of the interaction of three aliquots of Fe^0 powder (20, 100, or 200 g l^{-1}) with increasing $N\text{-}NO_3^-$ concentrations (from 0 to 45 mg l^{-1} of $N\text{-}NO_3^-$) are illustrated in Figure 2. An amount of 200 g l^{-1} iron is able to reduce $N\text{-}NO_3^-$ concentration below the European Union limit for drinking water (equal to 15 mg $N\text{-}NO_3^-$ l^{-1}) over the entire concentration range. However 100 g l^{-1} of iron were enough to completely reduce nitrate in the range $0 - 33$ mg l^{-1} of $N\text{-}NO_3^-$. Therefore the utilisation of a Fe dosage of 200 g l^{-1} would leave unexploited part of the material unless nitrate contamination is exceptionally high.

The increase in nitrate removal with increasing iron concentration was likely related to the increase in the reactive sites which were provided by the increased surface area of iron that passed from 14

$m^2 \, l^{-1}$ to 140 $m^2 \, l^{-1}$ by increasing the Fe^0 concentration from 20 g l^{-1} to 200 g l^{-1}. Nitrate, in fact, does not react with dissolved ferrous ions without catalysis of other transition-metal ions such as Cu^{2+} (Buresh, 1976) and Ag^+ (Brown, 1967), implying that abiotic reduction of nitrate occurs only at the surfaces of the iron metal, i.e. through a direct electron transfer from iron metal at the metal surface to the adsorbed oxidant (Su and Puls, 2004), (Zawaideh and Zhang, 1998), (Rodriguez-Maroto *et al.*, 2009).

Besides nitrate concentration, also nitrite and ammonium were measured at the end of the experiments. Results are reported in term of percentage of the initial $N\text{-}NO_3^-$ concentration (Figure 3). Nitrite was found in small amounts. Specifically, when using an iron concentration equal to 100 g l^{-1} and an initial $N\text{-}NO_3^-$ concentration from 2 to 33 mg l^{-1}, the amount of $N\text{-}NO_2^-$ was below the European Union limit for drinking water (0.1 mg $N\text{-}NO_2^-$ l^{-1}). When using 200 g l^{-1} iron $N\text{-}NO_2^-$ concentration was below the limit over the entire range of $N\text{-}NO_3^-$ addition. Ammonium was the dominant end product of nitrite reduction under our experimental conditions. Most of the added nitrate remained unreacted in all the samples with 20 g l^{-1} iron and, with 100 g l^{-1} iron, nearly one third of the nitrogen in the samples spiked with 45 mg l^{-1} was still found in the nitric form. At the end of the experiments the recovery of the initially added nitrogen was approximately 75-85%. Different studies suggest that gaseous species (N_2, N_2O, NO) may be formed in the reaction (Choe *et al.*, 2000), (Alowitz and Scherer, 2002), (Westerhoff and James, 2003), (Liou *et al.*, 2005), (Liou *et al.*, 2006). At alkaline pH and low Eh values (pH increased from 5.4 to >11 and Eh was ≤ -0.200 mV after the reaction occurrence) substantial amounts of N can be present in form of NH_3. Therefore the incomplete mass balance, in the present case, could be justified by the production of ammonia.
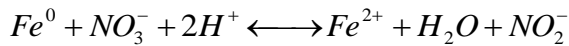
The aforementioned reaction products are consistent with the occurrence of the following reactions reported in the literature:

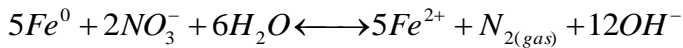- Ammonium generation from nitrate reduction:

$$4Fe^0 + NO_3^- + 10H^+ \longleftrightarrow 4Fe^{2+} + NH_4^+ + 3H_2O$$
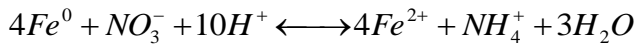
Eq. 3 (Alowitz and Scherer, 2002)

- Nitrite generation from nitrate reduction:

$$Fe^0 + NO_3^- + 2H^+ \longleftrightarrow Fe^{2+} + H_2O + NO_2^-$$

Eq. 4 (Siantar *et al.*, 1996), (Chew and Zhang, 1998), (Flis, 1991)

- N_2 production from nitrate reduction:
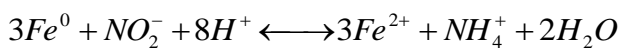
$$5Fe^0 + 2NO_3^- + 6H_2O \longleftrightarrow 5Fe^{2+} + N_{2(gas)} + 12OH^-$$

Eq. 5 (Choe *et al.*, 2000), (Chew and Zhang, 1998), (Flis, 1991), (Till *et al.*, 1998), (Kielemoes *et al.*, 2000)

$$10Fe^0 + 6NO_3^- + 3H_2O \longleftrightarrow 5Fe_2O_3 + 3N_{2(gas)} + 6OH^-$$
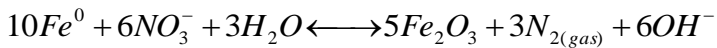
Eq. 6 (Siantar *et al.*, 1996), (Flis, 1991)

- Ammonium generation from nitrite reduction:

$$3Fe^0 + NO_2^- + 8H^+ \longleftrightarrow 3Fe^{2+} + NH_4^+ + 2H_2O$$

Eq. 7 (Alowitz and Scherer, 2002)

The variations of the nitrogen species with iron concentration is statistically significant (p-value below 0.001). It is worth noting that with increasing iron concentration not only ammonium increased and nitrate decreased, but also nitrite decreased. The result can be explained in terms of a higher amount of available reactive surface sites, which enabled not only a more complete transformation of nitrate into ammonium, but also a more complete reduction of nitrite through Eq. 7.

In all systems pH increased from 5.4 to >11 after the reaction occurrence, whereas Eh generally decreased reaching values of about -100 ÷ -200mV. The increase in pH probably results from iron corrosion by nitrate (Eq. 2) and from iron anaerobic corrosion in water:

$$Fe^0 + 2H_2O \longleftrightarrow Fe^{2+} + H_2 + 2OH^-$$
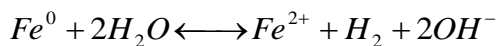
Eq. 8

According to (Rodríguez-Maroto *et al.*, 2009) both reactions can occur simultaneously in systems like the ones in this study.

Dissolved Fe^{2+} was recovered in remarkable amounts (up to 17 mg l^{-1}) only in the initial stages of the reaction. In groundwater, where the reaction rate is significantly slower compared with deionized water, the presence of Fe $^{2+}$ continued up to 20 hours. The presence of Fe^{2+} in the early stages of the reaction is consistent with the chemical reactions reported before. Equilibrium calculations (Chen *et al.*, 2004) indicate the presence of substantial amounts of Fe^{2+} ion for acid to neutral pH values. However it is likely that as reaction takes place, the system moves to a pH region (i.e. higher pH) where the stability of dissolved Fe^{2+} ions drastically decreases, whereas iron oxides become the dominant species. The formation of an oxide coating on Fe^0 particles was observed by means of FESEM-EDX analysis.

Figure 4 and Figure 5 reports FESEM images of unused iron material and of a sample from nitrate reduction experiment. The regular shape of the iron particles was lost after nitrate reduction, as platelets are formed onto the spherical particle surface. EDX analysis indicates that platelets are associated to a major amount of oxygen (about 10% atomic), therefore a relationship between composition and morphology is present. On the contrary in the case of unreacted iron, the percentage of oxygen was almost non detectable. In the literature (Sohn *et al.*, 2006) it is reported that the oxidation of nanoscale zerovalent iron particles involves the formation of crystalline

magnetite in a platelet shape. In the present case, the oxide formed after the reaction appeared as a coverage on the micrometric iron particles, apparently without a defined crystalline organization, rather than as discrete crystalline particles. Therefore depending on the conditions, the oxide will differ for type and crystalline organization, with consequences on their respective reactivity (Liu *et al.*, 2005).

The decrease of the rate of nitrate reduction with time observed in the kinetic experiments could be explained with the gradual formation of the aforementioned oxide coverage, which reduce the percentage of the sites available for nitrate reduction and hence the number of effective collisions per unit of time between the nitrate anions and the reactive sites on Fe surface.
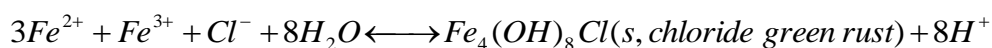
Nitrate reduction in groundwater. Nitrate reduction tests were repeated using a groundwater, in order to better understand the behaviour of iron particles under field conditions. According to the results obtained with deionized water, an iron concentration of 100 g l^{-1} was selected, while nitrate concentration ranged from 2 to 45 mg l^{-1} of N-NO$_3^-$ (like in experiments with deionized water).

A reaction time of 120 h was selected, to allow the reaching of quasi-equilibrium, as derived by the kinetic experiments (Figure 1). After this time the fast step of the reaction was completed and nearly 90% of the N-NO$_3^-$ reductable after two weeks was already removed. As shown in (Figure 6), in groundwater iron resulted to be less effective over the entire nitrate concentration range compared to deionized water (Figure 2), confirming the results of the kinetic experiments. Also in this case, the presence of organic matter and inorganic ions (i.e. sulphate, carbonate) in groundwater is likely to be responsible for the incomplete nitrate reduction, as such species are known to form inner-sphere complexes on the surface of Fe^0 and its corrosion products, blocking reactive sites for nitrate reduction (Su and Puls, 2004) and thus limiting the reaction
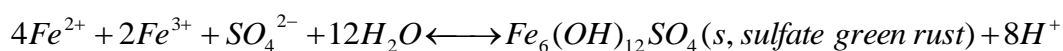
The reaction products were ammonium and unreacted nitrate, as in the case of deionized water (Figure 6), while nitrite was not detected. The pH recorded at the end of the experiment attained

lower values compared with deionized water (pH increased from 5.4 to about 7.5-8, instead of >11). At such pH values, ammonium, rather than ammonia, is the main nitrogen species. This could justify the fact that the recovery of the added nitrogen was complete, thus suggesting that gaseous nitrogen forms were not produced, differently from the case of deionized water. The Eh generally decreased reaching values of about -100 to -200 mV.

The presence of Fe^{2+} was not detectable in the experiments. As discussed previously for deionized water, at the aforementioned pH and Eh values, the main iron specie should be magnetite. Besides this specie, as the groundwater used contained chloride ion and sulphate ion, it is possible that green rust was also formed (Su and Puls, 2004):

$$3Fe^{2+} + Fe^{3+} + Cl^- + 8H_2O \longleftrightarrow Fe_4(OH)_8Cl(s, chloride\ green\ rust) + 8H^+$$

Eq. 9

$$4Fe^{2+} + 2Fe^{3+} + SO_4^{2-} + 12H_2O \longleftrightarrow Fe_6(OH)_{12}SO_4(s, sulfate\ green\ rust) + 8H^+$$

Eq. 10

Although not proven, the formation of green rust was suggested by the presence of a green film in the vials at the end of the reaction.

4.3. Ammonium adsorption on zeolitite

The dimensions of the utilized zeolitite material are heterogeneous, as particles from a few μm to tens of μm can be observed in FESEM images (Figure S 2 Supporting Informations). The superficial elements of raw zeolite according to EDX analysis are silicon and oxygen, and in minor amount aluminium, magnesium, potassium, calcium and iron. According to XRD analysis of zeolitite, such atoms are arranged in the main mineralogical forms of chabasite, micas and feldspars (Figure S 3).

Experimental data for ammonium adsorption on zeolitite are reported in Figure 7. The Freundlich equation gave a good fit to the data ($r^2 > 0.999$). The value of K in the Freundlich equation (Eq. 1) resulted 1.02 mg g^{-1} and the value of $1/n$ was 0.47.

Preliminary experiments showed that nitrate is not adsorbed by zeolitite. Therefore, when both iron and zeolitite are present, the decrease in nitrate concentration is likely to be caused only by iron reducing action, and not by zeolitite adsorption.

4.4. Ammonium adsorption on zeolitite after nitrate reduction

According to our results the zeolitite is able to adsorb ammonium, when added to a batch system of iron and nitrate in deionized water after the reduction. Out of the total 35 mg l-1 of $N-NO_3^-$ initially added to the system and reduced to ammonium by the zerovalent iron, less than 8 mgl^{-1} of N were recovered in solution after the interaction with the zeolitite. Ammonium adsorption after nitrate reduction was correctly predicted by the Freunlich isotherm obtained from adsorption experiments without iron addition, as can be observed in Figure 7 from the overlapping of the amounts of $N-NH_4^+$ adsorbed after reduction of $N-NO_3^-$ both in deionized water (white triangles) and in groundwater experiment (white circles) with the fitting line (Figure 7). This indicates that the ion exchange is not hindered by the presence of iron particles or by other competing species. Bivalent iron ions, produced as indicated in reactions mentioned in Eq. 3, Eq. 4 and Eq. 7, could compete with ammonium for adsorption, however, the bivalent form of iron was never detected in solution at the end of the nitrate reduction reaction. These results indicate that it is possible to remove nitrate from the solution using zerovalent iron and zeolitite, thus avoiding the permanence in solution of the NH_4^+ produced in the previous reaction.

In the experiments conducted with groundwater, when the nitrate reduction reaction reached a quasi-equilibrium, a residual amount of $N-NO_3^-$ was still present in the solution (about 4.5 mg l^{-1}). After adding the zeolitite, not only most of the ammonium was removed from the solution, but also

the N-NO$_3^-$, which concentration decreased from 4.5±0.36 mgl^{-1} to 0.13±0.01 mgl^{-1}. Like in the case of deionized water, ammonium adsorption followed quite well the Freundlich isotherm (Figure 7). We conclude that ammonium formed by nitrate reduction can be efficiently removed by means of adsorption onto zeolitite. Moreover the presence of zeolitite seems to favor the nitrate reduction. It is likely that as ammonium is removed from the solution by adsorption on zeolitite, the system will shift its equilibrium to compensate for the ammonium decrease in solution.

From the performance of zeolitite in groundwater, it can be deduced that its high NH$_4^+$ adsorbing capacity is maintained even when other cationic species are present. Therefore the method of nitrate reduction and subsequent ammonium adsorption is consistent with the application with groundwater.

5. Conclusions

Our laboratory results show that nitrate can be eliminated with the contemporary removal of the produced ammonium by means of sequential reactions with micrometric zerovalent iron and natural chabazite. The reactive material can be easily exploited in filters, while the use of Fe^0 in permeable reactive barriers for nitrate reduction would pose some additional challenges.

The nitrate reduction by zerovalent iron could determine the release of Fe^{2+} ion, which limit is 0.2 mg l^{-1} according to the European Union Council Directive 98/83/EC. In our experiments, this ionic species was not of concern, since it was detected only in the early stages of the reaction, as it was probably subsequently fixed on the oxidized particle surfaces. The nitrate reduction is also known, from the literature, to produce nitrite. Our experiments proved that the use of a sufficient amount of iron can minimize nitrite production, keeping its concentration below the safety limit. However, site-specific characteristics of groundwater should be taken into account while designing the filter, in order to select the appropriate dose of iron and zeolitite. Further experiments are required to

assess the suitability of the method to a wide range natural groundwaters differing in their chemical characteristics.

A future step of the research is to optimize the use of the spent adsorbent. The zeolitite could be either regenerated and the ammonia recovered could be reused, or the exausted zeolitite can be itself be used as a fertilizer and amendment for soils.

References

Alowitz, M.J., Scherer, M.M., 2002. Kinetics of Nitrate, Nitrite, and Cr(VI) Reduction by Iron Metal. Environmental Science & Technology 36, 299-306.

Bartsch, H., Ohshima, H., Shuker, D.E.G., Pignatelli, B., Calmels, S., 1990. Exposure of humans to endogenous N-nitroso compounds: implications in cancer etiology. Mutation Research/Reviews in Genetic Toxicology 238, 255-267.

Brown, L.L., Drury, J. S. , 1967. Nitrogen-isotope effects in the reduction of nitrate, nitrite, and hydroxylamine to ammonia. I. In sodium hydroxide solution with Fe(II). J. Chem. Phys. 46, 2833-2837.

Buresh, R.J., Moraghan, J. T., 1976. Chemical reduction of nitrate by ferrous iron. *J. Environ. Qual.* 5, 320-325.

Chen, S.S., Hsu, H.D., Li, C.W., 2004. A new method to produce nanoscale iron for nitrate removal. Journal of Nanoparticle Research 6, 639-647.
Chew, C.F., Zhang, T.C., 1998. In-situ remediation of nitrate-contaminated ground water by electrokinetics iron wall processes. Water Sci Technol 38, 135-142.

Choe, S., Chang, Y.Y., Hwang, K.Y., Khim, J., 2000. Kinetics of reductive denitrification by nanoscale zero-valent iron. Chemosphere 41, 1307-1311.

Choe, S., Liljestrand, H.M., Khim, J., 2004. Nitrate reduction by zero-valent iron under different pH regimes. Applied Geochemistry 19, 335-342.

Crooke, W.M.S., W.E. , 1971. Determination of ammonium in Kjeldahl digests of crops by an automated procedure. Journal of the Science of Food and Agriculture 22, 9-10.

European Council, 2001. Council Directive of 12 December 2001 concerning the protection of water against pollution caused by nitrates from agricultural sources In: Union, E. (Ed.). Official Journal L 375, 31/12/1991, pp. 0001 - 0008.

Flis, J., 1991. Stress corrosion cracking of structural steels in nitrate solutions. In: J. Flis, Editor, Corrosion of Metals and Hydrogen-Related Phenomena. Materials Science Monograph vol. 59, Elsevier, Amsterdam, NL (1991), pp. 57–94. Elsevier, Amsterdam, NL.

Follett, R.F., 2001. Nitrogen in the Environment: Sources, Problems, and Management., Amsterdam.

Gu, B.W., D.; Wu, L.; Phillips, D.; White, D.; Zhou, J., 2002. Microbiological Characteristics in a Zero-Valent Iron Reactive Barrier. Environmental Monitoring and Assessment </content/102878/?p=4b023382ac044f909b15a0416fe36ffa&pi=0> 77, 293-309.

Hallberg, G.R.a.K., D.R., 1993. Regional Ground-water Quality. Van Nostrand Reinhold, New York.

Huang, C.-P., Wang, H.-W., Chiu, P.-C., 1998. Nitrate reduction by metallic iron. Water Research 32, 2257-2264.

Huang, Y., Mou, S.-f., Riviello, J.M., 2000. Determination of ammonium in seawater by column-switching ion chromatography. Journal of Chromatography A 868, 209-216.
Joossens, J.V., Hill, M.J., Elliott, P., Stamler, R., Stamler, J., Lesaffre, E., Dyer, A., Nichols, R.,

Kesteloot, H., PREVENTION, O.B.O.E.C., THE INTERSALT COOPERATIVE RESEARCH GROUP, 1996. Dietary Salt, Nitrate and Stomach Cancer Mortality in 24 Countries. Int. J. Epidemiol. 25, 494-504.

Kielemoes, J., De Boever, P., Verstraete, W., 2000. Influence of Denitrification on the Corrosion of Iron and Stainless Steel Powder. Environmental Science & Technology 34, 663-671.

Li, X.Q., Elliott, D.W., Zhang, W.X., 2006. Zero-valent iron nanoparticles for abatement of environmental pollutants: Materials and engineering aspects. Critical Reviews in Solid State and Materials Sciences 31, 111-122.

Liang B. C., M., A.F. , 1994. Corn yield, nitrogen uptake and nitrogen use efficiency as influenced by nitrogen fertilization. Can. J. Soil Sci. 74, 235-240.
Liou, Y.H., Lo, S.-L., Kuan, W.H., Lin, C.-J., Weng, S.C., 2006. Effect of precursor concentration on the characteristics of nanoscale zerovalent iron and its reactivity of nitrate. Water Research 40, 2485-2492.

Liou, Y.H., Lo, S.-L., Lin, C.-J., Kuan, W.H., Weng, S.C., 2005. Chemical reduction of an unbuffered nitrate solution using catalyzed and uncatalyzed nanoscale iron particles. Journal of Hazardous Materials 127, 102-110.

Liu, C., Huang, P.M., 2003. Kinetics of lead adsorption by iron oxides formed under the influence of citrate. Geochimica et Cosmochimica Acta 67, 1045-1054.

Liu, Y., Choi, H., Dionysiou, D., Lowry, G.V., 2005. Trichloroethene Hydrodechlorination in Water by Highly Disordered Monometallic Nanoiron. Chemistry of Materials 17, 5315-5322.

Loeppert, R.H., Inskeep, W.P., 1996. Methods of soil analysis. Part 3. Chemical methods. . Madison, WI, USA. .

Martin, M., Yu, G., Barberis, E., Violante, A., Kozak, L.M., Huang, P.M., 2009. Impact of Structural Perturbation of Aluminum Hydroxides by Tannate on Arsenate Adsorption. Soil Sci Soc Am J 73, 1664-1675.

Molfetta, A., Sethi, R., 2006. Clamshell excavation of a permeable reactive barrier. Environmental Geology 50, 361-369.

Noubactep, C., Caré, S., Enhancing sustainability of household water filters by mixing metallic iron with porous materials. Chemical Engineering Journal In Press, Corrected Proof.

Passaglia, E., 2008. Zeoliti naturali, zeolititi e loro applicazioni. Venezia-Italy.

Passaglia, E., Marchi, E., La Rocca, D., 1999. *Removal of NH$_4$ from wastewaters using Italian zeolitites*. Materials Engineering 10, 269-282.

Rahman, A., Agrawal, A., , 1997. Reduction of nitrate and nitrite by iron metal :Implications for groundwater remediation. Preprint extended abstract, Division of Environmental Chemistry, Am. Chem. Soc., San Francisco, CA, 213 (175-ENVR part 1) 13–17 April, 37(1), pp. 157–159.

Rodriguez-Maroto, J.M., Garcia-Herruzo, F., Garcia-Rubio, A., Gomez-Lahoz, C., Vereda-Alonso, C., 2009. Kinetics of the chemical reduction of nitrate by zero-valent iron. Chemosphere 74, 804-809.

Rodríguez-Maroto, J.M., García-Herruzo, F., García-Rubio, A., Gómez-Lahoz, C., Vereda-Alonso, C., 2009. Kinetics of the chemical reduction of nitrate by zero-valent iron. Chemosphere 74, 804-809.

Saha, U.K., Liu, C., Kozak, L.M., Huang, P.M., 2004. Kinetics of Selenite Adsorption on Hydroxyaluminum- and Hydroxyaluminosilicate-Montmorillonite Complexes. Soil Sci Soc Am J 68, 1197-1209.

Saha, U.K., Liu, C., Kozak, L.M., Huang, P.M., 2005. Kinetics of selenite desorption by phosphate from hydroxyaluminum- and hydroxyaluminosilicate-montmorillonite complexes. Geoderma 124, 105-119.

Schaefer, C.E., Fuller, M.E., Condee, C.W., Lowey, J.M., Hatzinger, P.B., 2007. Comparison of biotic and abiotic treatment approaches for co-mingled perchlorate, nitrate, and nitramine explosives in groundwater. Journal of Contaminant Hydrology 89, 231-250.

Shannon, M.A., Bohn, P.W., Elimelech, M., Georgiadis, J.G., Marinas, B.J., Mayes, A.M., 2008. Science and technology for water purification in the coming decades. Nature 452, 301-310.

Shin, K.-H., Cha, D.K., 2008. Microbial reduction of nitrate in the presence of nanoscale zero-valent iron. Chemosphere 72, 257-262.

Siantar, D.P., Schreier, C.G., Chou, C.S., Reinhard, M., 1996. Treatment of 1,2-dibromo-3-chloropropane and nitrate-contaminated water with zero-valent iron or hydrogen/palladium catalysts. Water Research 30, 2315-2322.

Sobsey, M.D., Stauber, C.E., Casanova, L.M., Brown, J.M., Elliott, M.A., 2008. Point of Use Household Drinking Water Filtration: A Practical, Effective Solution for Providing Sustained Access to Safe Drinking Water in the Developing World. Environmental Science & Technology 42, 4261-4267.

Sohn, K., Kang, S.W., Ahn, S., Woo, M., Yang, S.K., 2006. Fe(0) nanoparticles for nitrate reduction: Stability, reactivity, and transformation. Environmental Science & Technology 40, 5514-5519.

Su, C.M., Puls, R.W., 2004. Nitrate reduction by zerovalent iron: Effects of formate, oxalate, citrate, chloride, sulfate, borate, and phosphate. Environmental Science & Technology 38, 2715-2720.

Till, B.A., Weathers, L.J., Alvarez, P.J.J., 1998. Fe(0)-Supported Autotrophic Denitrification. Environmental Science & Technology 32, 634-639.

Wang, Y., Lin, F., Pang, W., 2008. Ion exchange of ammonium in natural and synthesized zeolites. Journal of Hazardous Materials 160, 371-375.

Weber, E.J., 1996. Iron-Mediated Reductive Transformations:â€‰ Investigation of Reaction Mechanism. Environmental Science & Technology 30, 716-719.

Westerhoff, P., James, J., 2003. Nitrate removal in zero-valent iron packed columns. Water Research 37, 1818-1830.

Yang, G.C.C., Lee, H.-L., 2005. Chemical reduction of nitrate by nanosized iron: kinetics and pathways. Water Research 39, 884-894.

Yu, G., Saha, U.K., Kozak, L.M., Huang, P.M., 2006. Kinetics of cadmium adsorption on aluminum precipitation products formed under the influence of tannate. Geochimica et Cosmochimica Acta 70, 5134-5145.

Zawaideh, L.L., Zhang, T.C., 1998. The effects of pH and addition of an organic buffer (HEPES) on nitrate transformation in Fe[0]-water systems. IWA Publishing, London, ROYAUME-UNI.

The Drinking Water Directive (DWD), Council Directive 98/83/EC, Available at http://ec.europa.eu/environment/water/water-drink/index_en.html

Captions

Table 1 Rate constants (K), specific surface area normalized rate constants (KSSA), r2 and p values for pseudo-first-order equation fitted to the kinetic data of nitrate reduction.
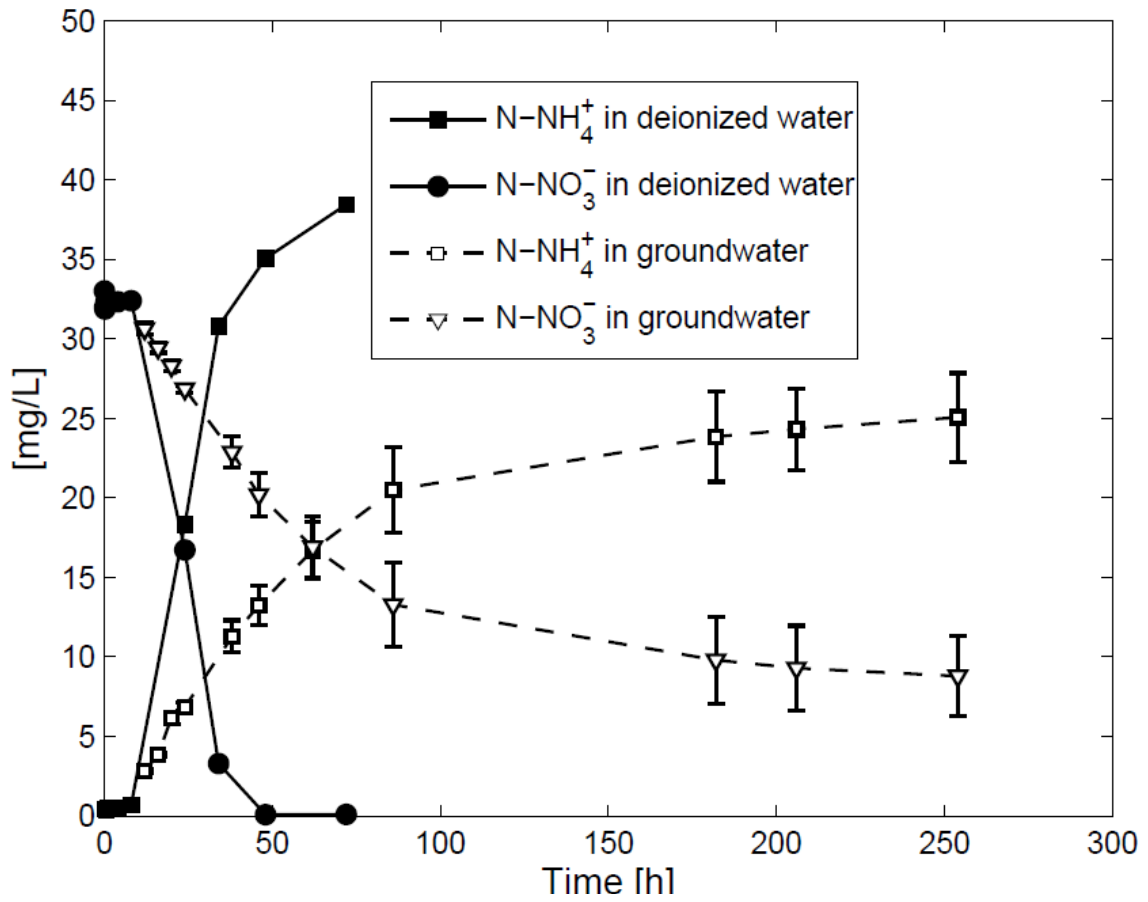
Figure 1 Experimental NO_3^- removal and NH_4^+ generation. Results are reported as mean value (points) and standard error (error bars).
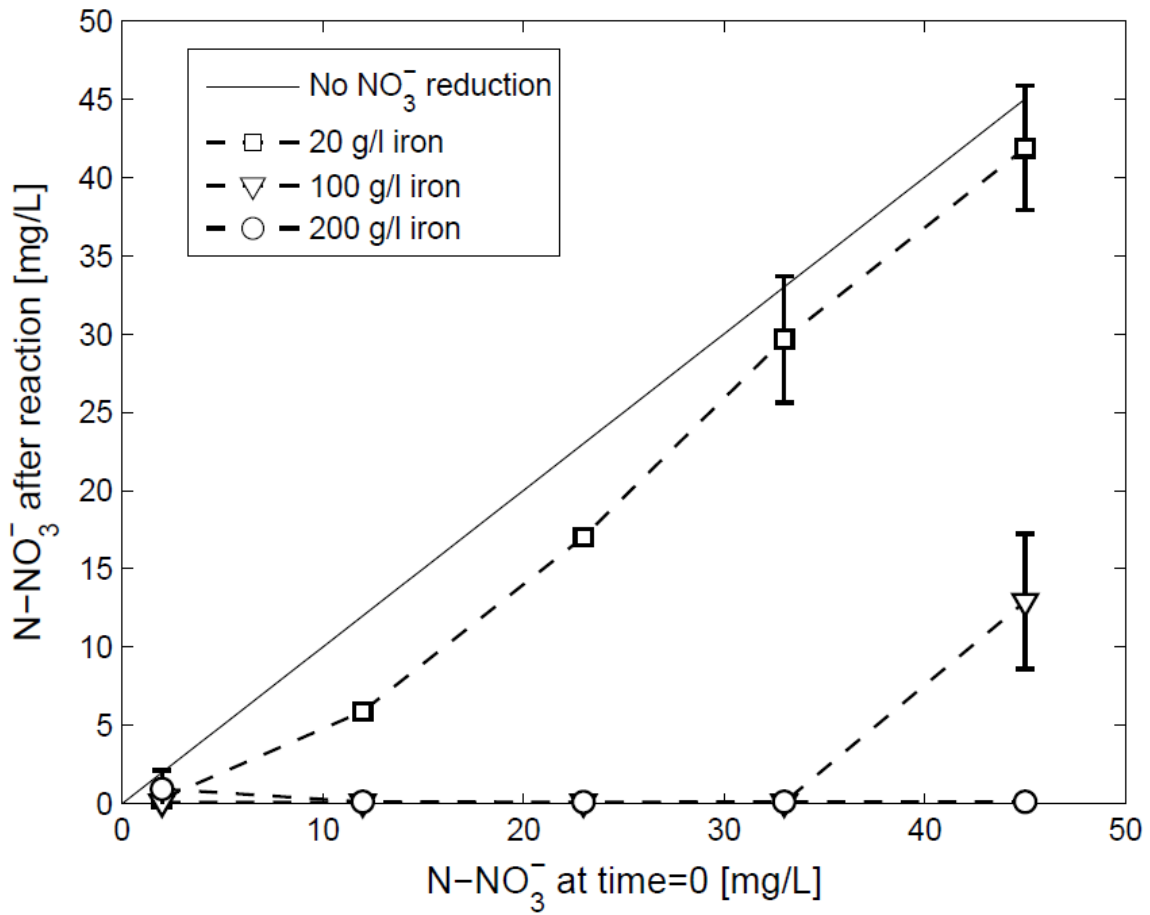
Figure 2 Concentration of nitrate in solution at the end of 40 h experiment as a function of the initial nitrate concentration, with different iron amounts in deionized water.
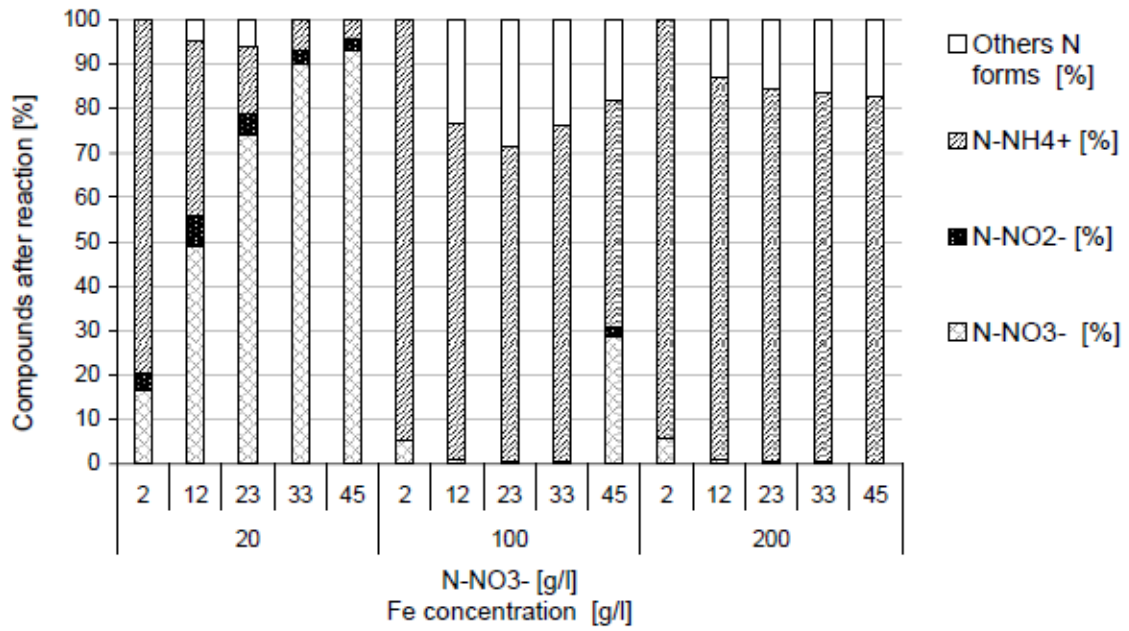
Figure 3 Nitrogen mass balance for experiments in deionized water with an iron concentration of 20 g/l. Each experiment is reported as average value.
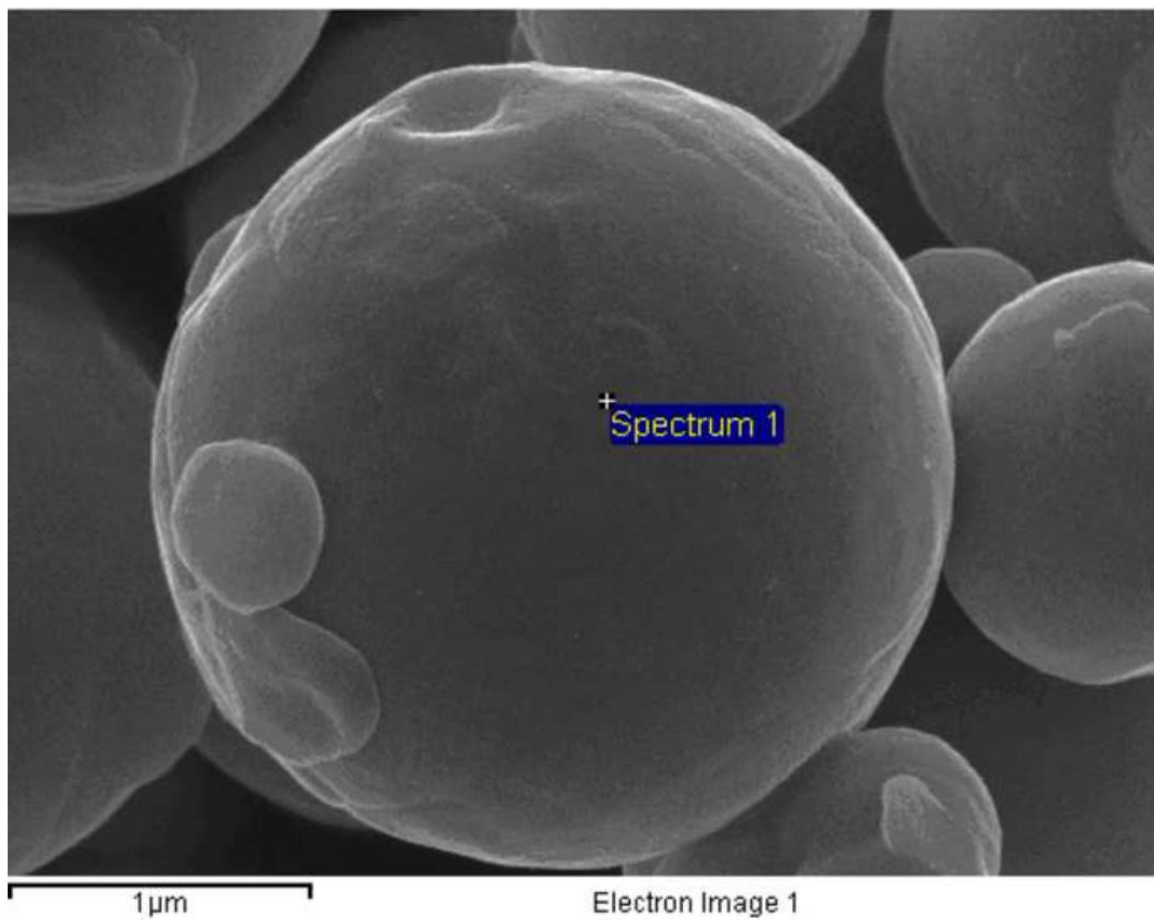
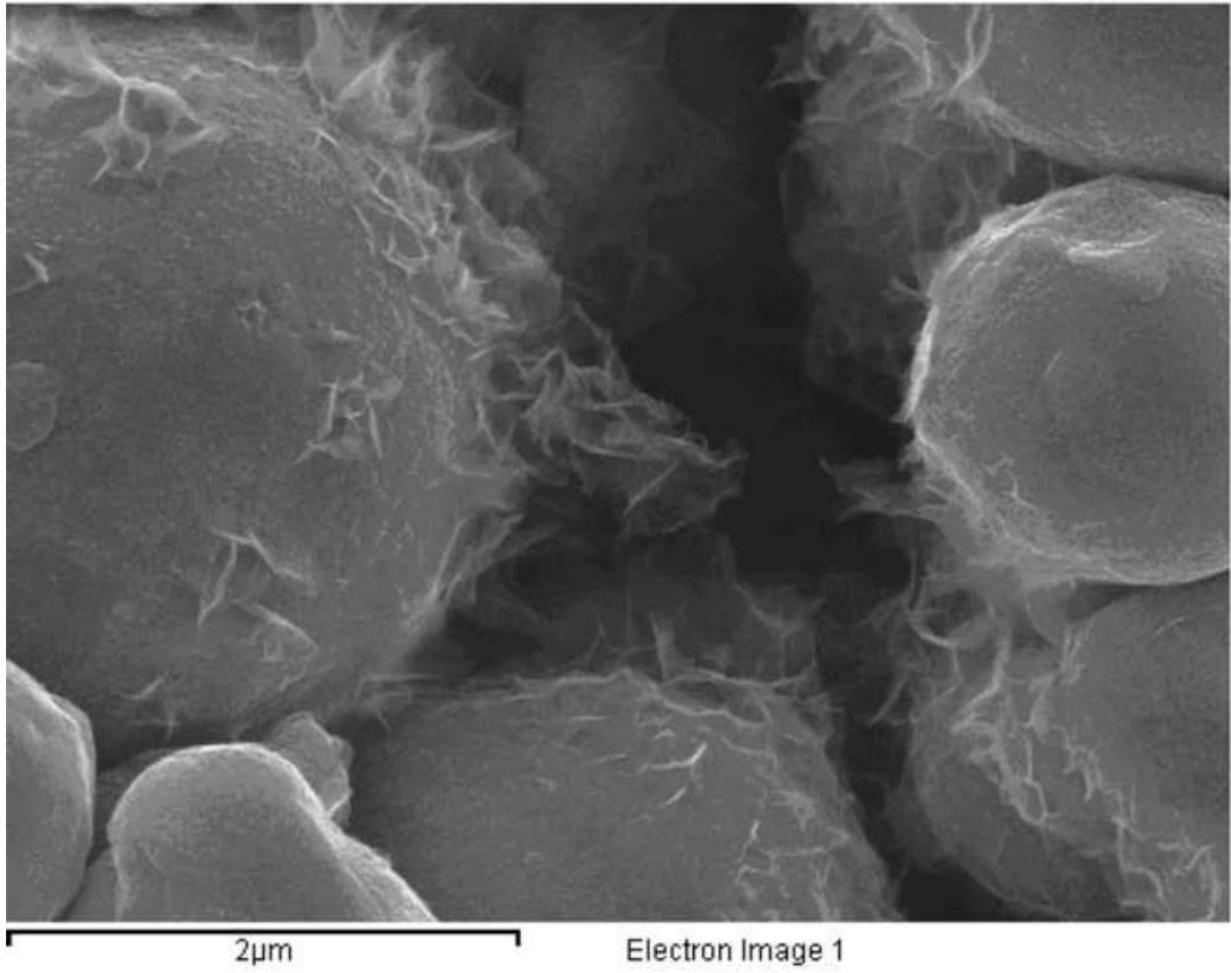Figure 4 FESEM image of unreacted iron particle.

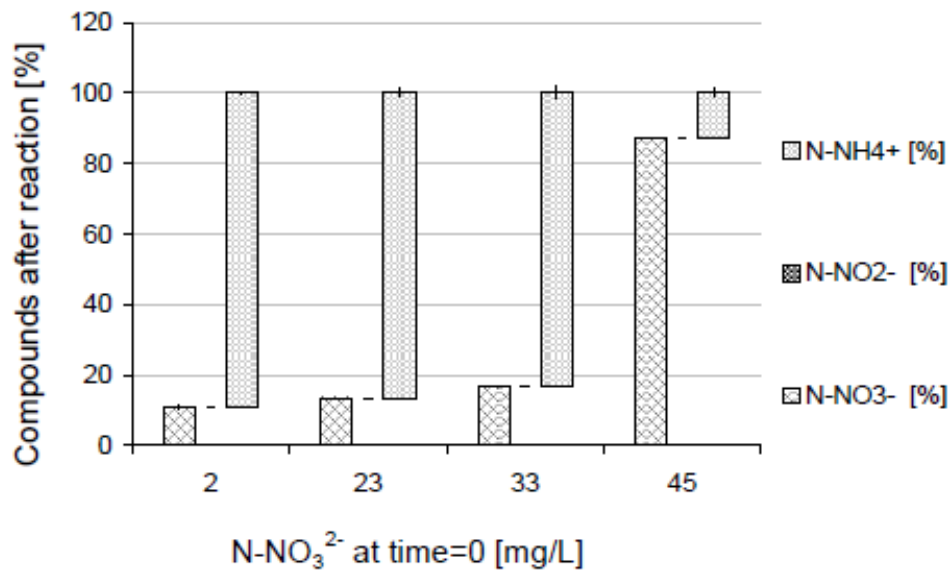Figure 5 FESEM image of iron material after nitrate reduction in deionized water.

Figure 6 Nitrogen mass balance for experiments in groundwater with an iron concentration of 100 g/l. Each experiment is reported as average value and standard deviation.

Figure 7 Amount of ammonium ion adsorbed per unit weight of zeolitite (Q) vs equilibrium amount in solution (black squares) and fitting with the Freundlich model (black line). The solid/solution partition of ammonium deriving from nitrate reduction experiments in deionized water (white triangles) and groundwater (white circles) is also reported.

Figure 1. Experimental NO₃⁻ removal and NH₄⁺ generation. Results are reported as mean value (points) and standard error (error bars).

Figure 2 Concentration of nitrate in solution at the end of 40 h experiment as a function of the initial nitrate concentration, with different iron amounts in deionized water.

Figure 3 Nitrogen mass balance for experiments in deionized water with an iron concentration of 20 g/l. Each experiment is reported as average value.

Figure 4 FESEM image of unreacted iron particle.

Figure 5 FESEM image of iron material after nitrate reduction in deionized water.

Figure 6 Nitrogen mass balance for experiments in groundwater with an iron concentration of 100 g/l. Each experiment is reported as average value and standard deviation.
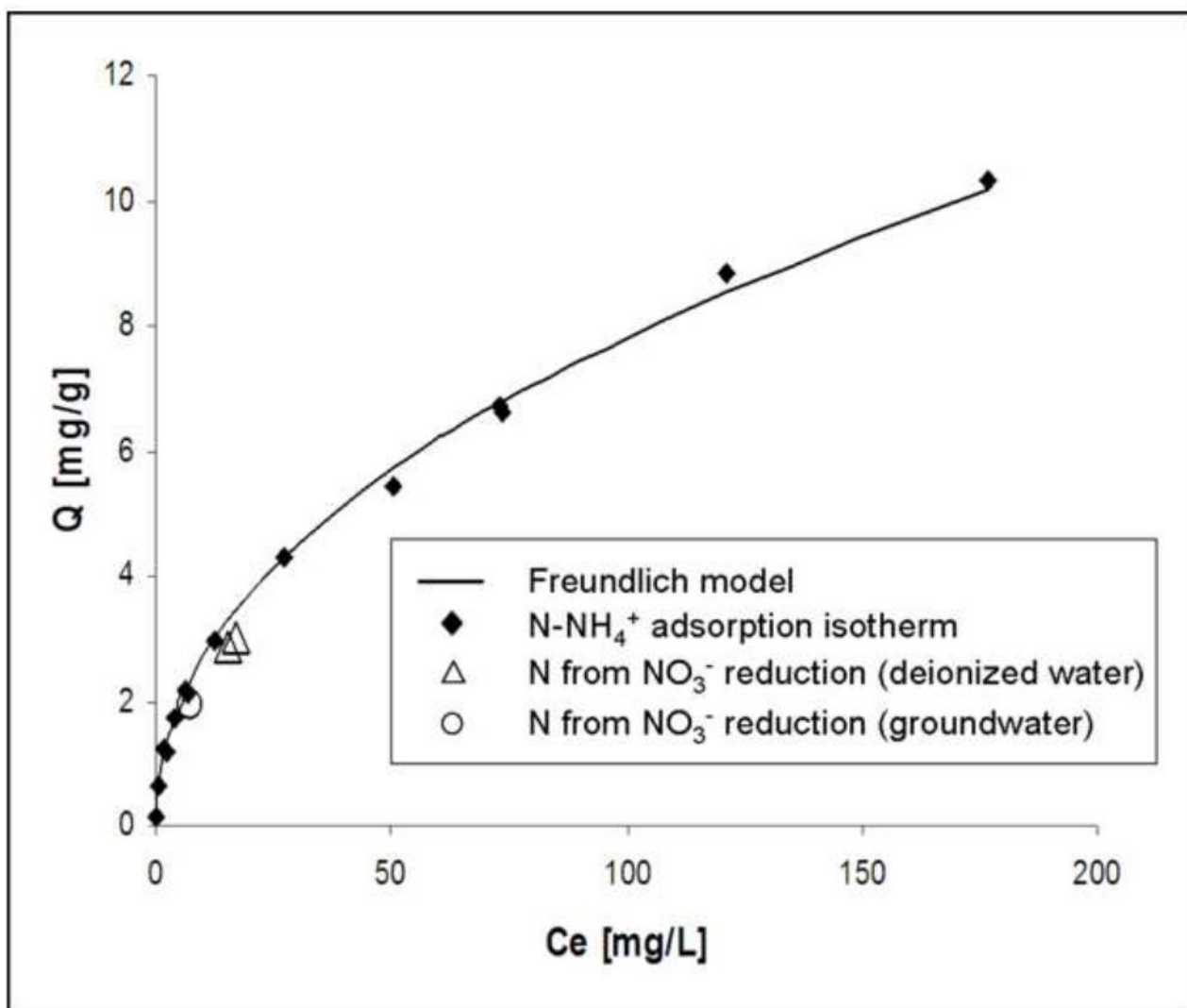
Figure 7 Amount of ammonium ion adsorbed per unit weight of zeolitite (Q) vs equilibrium amount in solution (black squares) and fitting with the Freundlich model (black line). The solid/solution partition of ammonium deriving from nitrate reduction experiments in deionized water (white triangles) and groundwater (white circles) is also reported.

Table 1 Rate constants (K), specific surface area normalized rate constants (KSSA), r2 and p values for pseudo-first-order equation fitted to the kinetic data of nitrate reduction.

	K (h^{-1})	K_{SSA} $(h^{-1} \, m^{-2} \, ml)$	r^2	p
Deionized water	0.108	1.5	0.844	0.028
Groundwater Fast reaction	0.012	0.164	0.998	<0.001
Groundwater Slow reaction	0.003	0.037	0.954	0.023

Supplementary Material

Reduction of nitrate and ammonium adsorption using microscale iron particles and zeolitite

Silvia Comba[a], Maria Martin[b], Daniele Marchisio[a], Rajandrea Sethi[a], Elisabetta Barberis [b]

[a] DITAG – Dipartimento del Territorio, dell'Ambiente e delle Geotecnologie, Politecnico di Torino, Torino, Italy.

[b] Di.Va.P.R.A. - Dipartimento di Valorizzazione e Protezione delle Risorse Agroforestali, Facoltà di Agraria, Università di Torino, Italy

Table S 1 Chemical composition of the sampled groundwater. Standard deviation was always below 2%

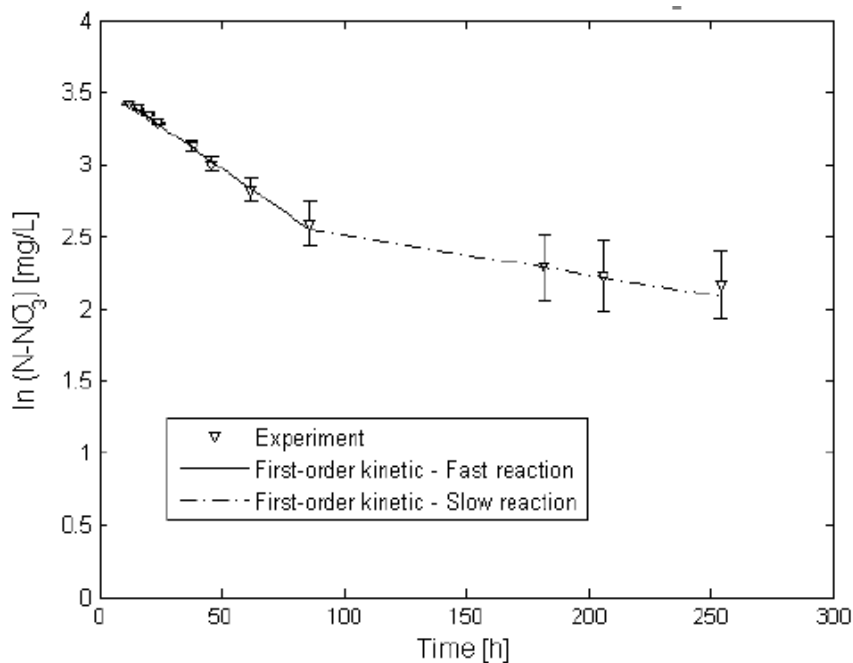|	
pH	6.96
N-N0$_3^-$ [mg l^{-1}]	0.23
N-N0$_2^-$ [mg l^{-1}]	< 0.05
N-NH$_4^+$ [mg l^{-1}]	< 0.10
Cl$^-$ [mg l^{-1}]	23.43
S0$_4^{2-}$ [mg l^{-1}]	75.44
P0$_4^{3-}$ [mg l^{-1}]	<0.05
CO$_3^{2-}$ [mg l^{-1}]	200
TOC [mg l^{-1}]	1.56

Figure S 1 Experimental NO$_3^-$ removal in groundwater as a function of time and fitting with pseudo-first order equation.
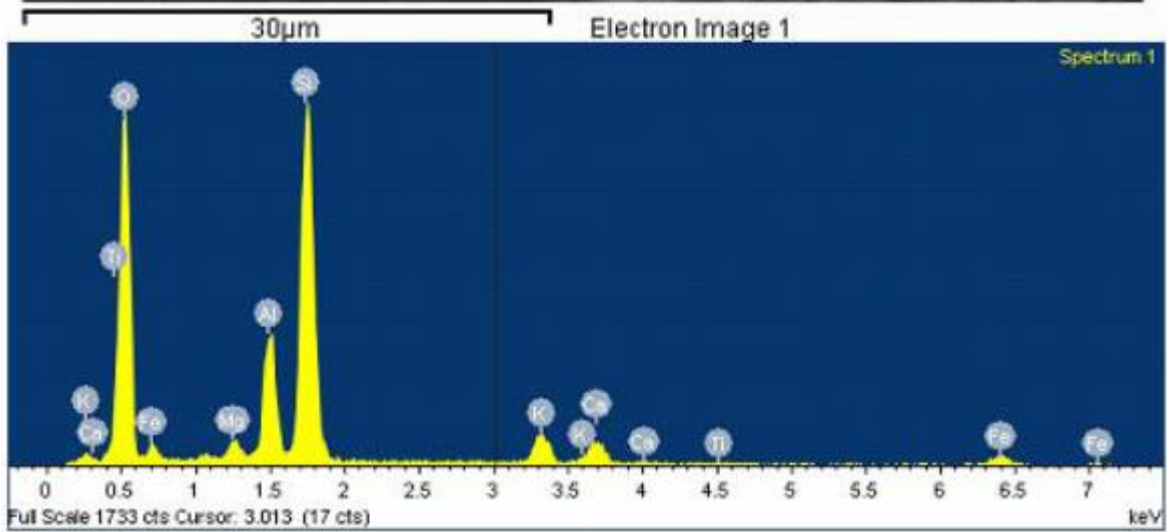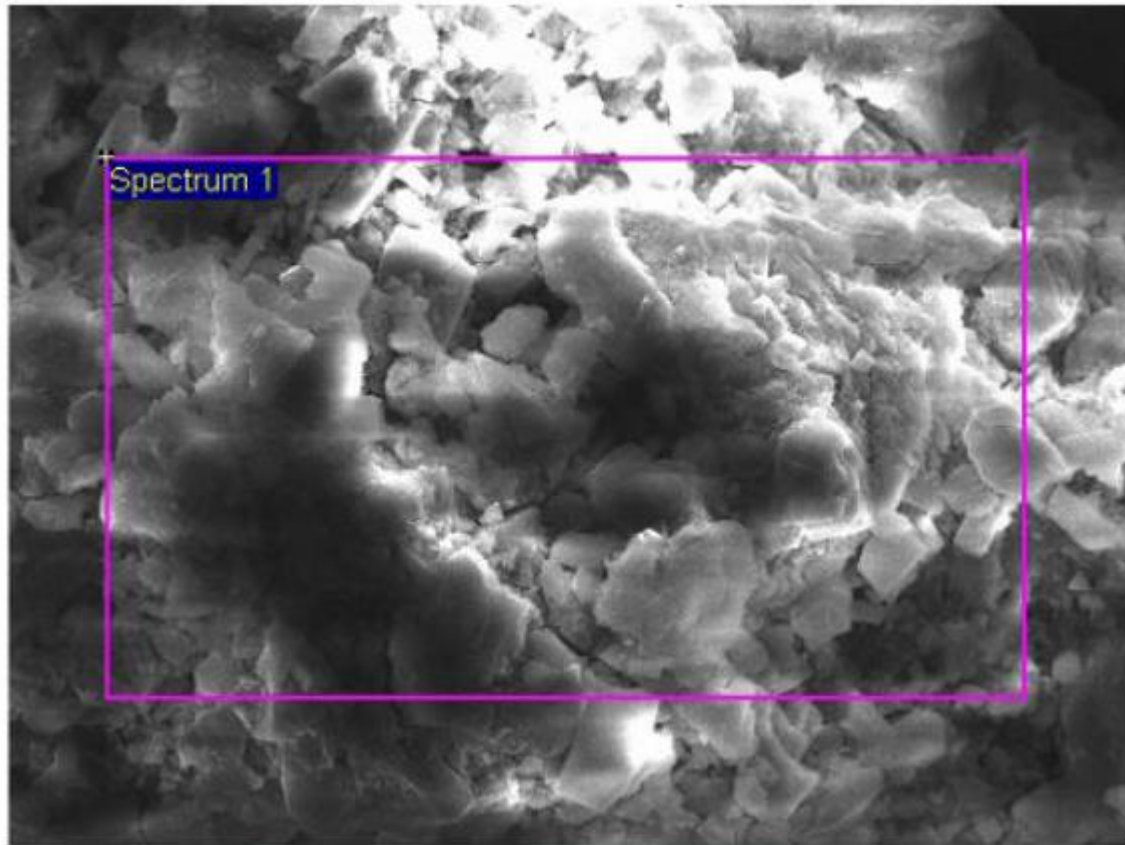
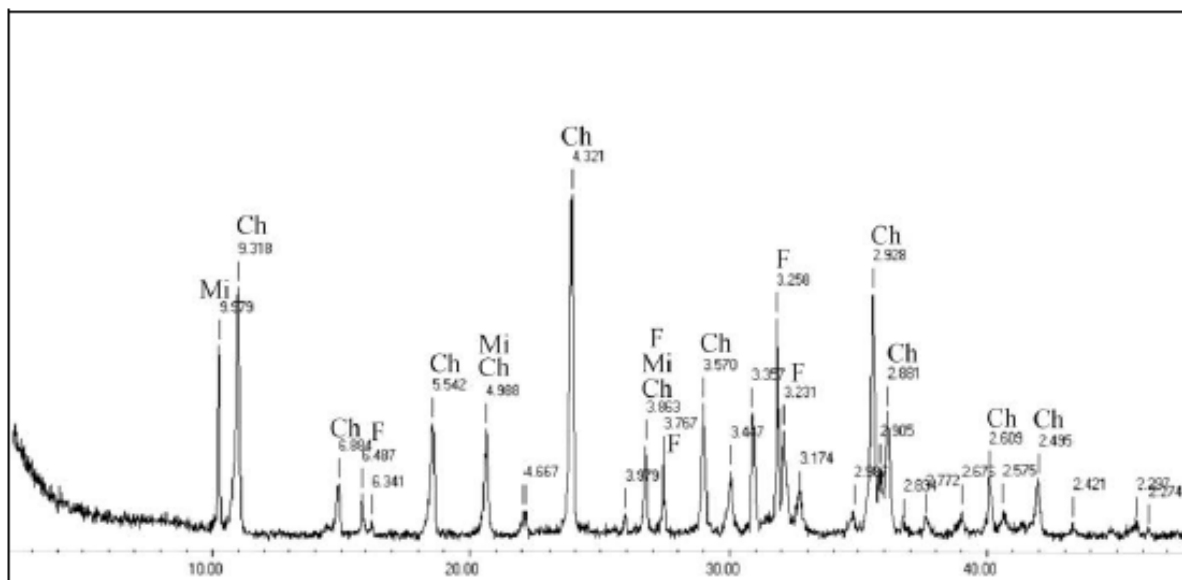Figure S2. FESEM image and EDX analysis of the zeolitite sample.

Figure S 3. XRD patterns of the zeolitite sample.